

Rotating magnetoelectric effect in a ground state of a coupled spin-electron model on a doubly decorated square lattice

Hana Čenčariková^{a,*}, Jozef Strečka^b

^a*Institute of Experimental Physics, Slovak Academy of Sciences, Watsonova 47, 040 01 Košice, Slovakia*

^b*Department of Theoretical Physics and Astrophysics, Faculty of Science, P. J. Šafárik University, Park Angelinum 9, 040 01 Košice, Slovakia*

Abstract

Exact analytical calculations are performed to study the rotating magnetoelectric effect in a ground state of a coupled spin-electron model on a doubly decorated square lattice with and without presence of an external magnetic field. Novel spatially anisotropic magnetic ground states emergent due to a rotation in an external electric field are found at three physically interesting electron concentrations ranging from a quarter up to a half filling. In absence of the magnetic field existence of spatially anisotropic structures requires a fractional electron concentration, where a significant influence of spatial orientation of an electric field is observed. It turns out that the investigated model exhibits a rotating magnetoelectric effect at all three concentrations with one or two consecutive critical points in presence of magnetic field. At the same time, the rotating electric field has a significant effect on a critical value of an electrostatic potential, which can be enhanced or lowered upon changing the electron hopping and the magnitude of an applied magnetic field. Finally, we have found an intriguing interchange of magnetic order between the horizontal and vertical directions driven by a rotation of the electric field, which is however destabilized upon strengthening of the magnetic field.

Keywords: Classical spin models, Rotating magnetoelectric effect, Exact analytical calculations, Phase transitions

1. Introduction

The study of the magnetoelectric effect as well as materials with an electric-field controlled magnetism has been a subject of the longstanding interest in the condensed matter physics. At the beginning the concerns of researchers in this field were attracted only sporadically, however, the discovery of novel functional materials [1–3] has a dramatic enhancement of researcher interest in this specific area [4]. The main reason of such expansion relates to a wide range of practical applications, e.g., in the spintronics, automation engineering, security, navigation or medicine [5–12] and also lies in a necessity to deeper understand the processes responsible for the unconventional properties of these functional materials. Another motivation for enhanced research activities in this specific area is based on a requirement to find novel low-energy consuming and/or eco-friendly mechanisms preserving a functional character of used materials.

In the present paper we would like to extend our previous study, where the novel concept about the rotating magnetoelectric effect has been introduced [13]. Our considerations have been based on the analogy with a recent discovery of a rotating magnetocaloric effect, where the cooling or heating is achieved through a spatial rotation of the sample in a constant magnetic field instead of its moving in and out of a magnet or by actively changing the magnetic field [2]. As was shown during next few years, the rotary magnetic refrigeration observed in various anisotropic magnetic materials is technically more convenient and effective in comparison to its conventional counterpart [14–20]. Based on this idea we have applied an external electric field along the arbitrary spatial direction lying in the plane of two-dimensional (2D) half-filled spin-electron system and we have observed that spatially modulated influence of an electric field on

*Corresponding author:

Email address: hcencar@saske.sk (Hana Čenčariková)

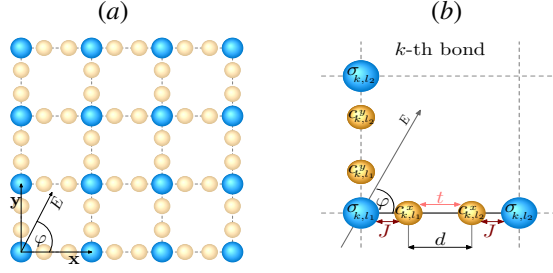


Figure 1: A schematic representation of a coupled spin-electron system on a 2D doubly decorated square lattice (a) supplemented with a specific detail of the k -th unit cell (b). Large (blue) balls represent the location of Ising spins and small (yellow) balls denote the location of decorating sites over which the mobile electrons are delocalized. All relevant interactions entering into the model Hamiltonian are also visualized.

charged particles significantly influences the critical temperature of an investigated 2D system [13]. The detection of a substantial rotating magnetoelectric effect at a half filling motivated us to investigate an identical spin-electron model in other physically interesting electron concentrations to complement a rich spectrum of its unconventional properties [21–23]. Our further analyses will be exclusively limited to an investigation of a zero-temperature rotating magnetoelectric effect, which allows to examine it in the most authentic manner without the side effect of thermal fluctuations.

The outline of this paper is as follows. In Sec. 2 we will briefly introduce an investigated model together with a method used to study the rotating magnetoelectric effect. The most interesting results demonstrating existence of the aforementioned phenomenon with and without the influence of external magnetic field will be detailed discussed in Sec. 3. Finally, the summary of the scientifically most significant achievements will be mentioned in Sec. 4.

2. Model and Method

The investigated coupled spin-electron model on a doubly decorated square lattice consists of localized Ising spins $\hat{\sigma}^z$ with two possible eigenvalues $\sigma^z = \pm 1$ and the mobile electrons delocalized over all bonds lying in between two nearest-neighbor Ising spins as displayed in Fig. 1. The local character of all present interactions allows us to decompose the total Hamiltonian $\hat{\mathcal{H}}$ into the N horizontal ($\hat{\mathcal{H}}_k^x$) and N vertical ($\hat{\mathcal{H}}_k^y$) bond Hamiltonians, which can be defined through the following formula

$$\begin{aligned} \hat{\mathcal{H}}_k^\delta = & -t(\hat{c}_{k,l_1,\uparrow}^{\dagger,\delta}\hat{c}_{k,l_2,\uparrow}^\delta + \hat{c}_{k,l_1,\downarrow}^{\dagger,\delta}\hat{c}_{k,l_2,\downarrow}^\delta + h.c.) - \sum_{\alpha=1,2} (J\hat{\sigma}_{k,l_\alpha}^{z,\delta} + h)(\hat{n}_{k,l_\alpha,\uparrow}^\delta - \hat{n}_{k,l_\alpha,\downarrow}^\delta) \\ & - \sum_{\alpha=1,2} \left[\frac{h}{4}\hat{\sigma}_{k,l_\alpha}^{z,\delta} - (-1)^\alpha V_\delta \sum_{\gamma=\uparrow,\downarrow} \hat{n}_{k,l_\alpha,\gamma}^\delta \right] - \mu\hat{n}_k^\delta, \end{aligned} \quad (1)$$

where $\delta = x, y$ and $\hat{c}_{k,l_\alpha,\gamma}^{\dagger,\delta}$, $\hat{c}_{k,l_\alpha,\gamma}^\delta$ ($\alpha = 1, 2$; $\gamma = \uparrow, \downarrow$) denote the creation and annihilation fermionic operators of the mobile electrons from the k -th bond with the respective number operators $\hat{n}_{k,l_\alpha,\gamma}^\delta = \hat{c}_{k,l_\alpha,\gamma}^{\dagger,\delta}\hat{c}_{k,l_\alpha,\gamma}^\delta$ determining occupation of a decorating site l_α through a mobile electron with a spin γ . The sum of all partial number operators $\hat{n}_{k,l_\alpha,\gamma}^\delta$ commonly defines the total number operator at k -th bond, $\hat{n}_k^\delta = \sum_{\alpha=1,2} (\hat{n}_{k,l_\alpha,\uparrow}^\delta + \hat{n}_{k,l_\alpha,\downarrow}^\delta)$. The relevant interactions entering into the horizontal as well as vertical bond Hamiltonians (1) correspond to the kinetic energy of mobile electrons modulated by the hopping amplitude t , the Ising-type exchange interaction J between the nearest-neighbor localized Ising spins and mobile electrons. Parameters h and V_δ take into account an influence of the external magnetic and electric fields, respectively. While the magnetic field affects simultaneously electron as well as spin subsystem, the electric field E acts exclusively on the subsystem of mobile electrons with a charge $|e|$. Imposing the distance d between nearest-neighbor decorating sites allows us to unambiguously determine the magnitude of the electrostatic potential V ($V = E|e|d/2$). The difference between the horizontal and vertical bond Hamiltonians (1) originates from a different

contribution of the electrostatic potential V on the horizontal (V_x) and vertical (V_y) bonds, which can be easily tuned upon varying an inclination of the electric field from the global frame axis x , as determined by the polar angle φ (see Fig. 1). Owing to this fact, the horizontal and vertical contribution of the electrostatic energy can be expressed as $V_x = V \cos \varphi$ and $V_y = V \sin \varphi$, respectively. The last term μ entering into the Eq. (1) is the standard chemical potential, which controls the number of mobile electrons per bond.

In order to analyze the rotating magnetoelectric effect at zero temperature we have at first determined the magnetic phase diagrams as a function of the polar angle φ . The energy of each magnetic configuration entering into the ground-state phase diagram is defined as a sum of the lowest-energy eigenstates over all N pairs of bonds in the horizontal ($\varepsilon_{k_i}^x, i = 1, 2, \dots, 16$) and vertical ($\varepsilon_{k_i}^y, i = 1, 2, \dots, 16$) direction, $\varepsilon = \sum_{k=1}^N (\varepsilon_k^x + \varepsilon_k^y)$. It should be mentioned that the electron occupation $\langle \hat{n}_k^\delta \rangle$ can be different for two orthogonal spatial directions. Since the different occupation number $\langle \hat{n}_k^\delta \rangle$ is allowed, it is convenient to define the mean electron concentration ρ through the relation $\rho = (\langle \hat{n}_k^x \rangle + \langle \hat{n}_k^y \rangle)/2$. The lowest-energy eigenstates in both spatial directions can be derived from the sixteen energy eigenvalues $\varepsilon_{k_i}^\delta (i = 1, 2, \dots, 16)$ obtained by an exact diagonalization procedure (reported in detail in Ref. [24]) for all available configurations of Ising spins σ_{k,l_1}^δ and σ_{k,l_2}^δ

$$\begin{aligned}
\langle \hat{n}_k^\delta \rangle = 0 : \varepsilon_{k_1}^\delta &= -\frac{h}{2} A_+^\delta, \\
\langle \hat{n}_k^\delta \rangle = 1 : \varepsilon_{k_2, k_3}^\delta &= -(JA_+^\delta + h) - \frac{h}{2} A_+^\delta \mp B_+^\delta - \mu, \\
&: \varepsilon_{k_4, k_5}^\delta = (JA_+^\delta + h) - \frac{h}{2} A_+^\delta \mp B_-^\delta - \mu, \\
\langle \hat{n}_k^\delta \rangle = 2 : \varepsilon_{k_6, k_7}^\delta &= \mp 2(JA_+^\delta + h) - \frac{h}{2} A_+^\delta - 2\mu, \\
&: \varepsilon_{k_8, k_9}^\delta = -C_\pm^\delta - \frac{h}{2} A_+^\delta - 2\mu, \\
&: \varepsilon_{k_{10}, k_{11}}^\delta = C_\pm^\delta - \frac{h}{2} A_+^\delta - 2\mu, \\
\langle \hat{n}_k^\delta \rangle = 3 : \varepsilon_{k_{12}, k_{13}}^\delta &= -(JA_+^\delta + h) - \frac{h}{2} A_+^\delta \pm B_-^\delta - 3\mu, \\
&: \varepsilon_{k_{14}, k_{15}}^\delta = (JA_+^\delta + h) - \frac{h}{2} A_+^\delta \pm B_+^\delta - 3\mu, \\
\langle \hat{n}_k^\delta \rangle = 4 : \varepsilon_{k_{16}}^\delta &= -\frac{h}{2} A_+^\delta - 4\mu.
\end{aligned} \tag{2}$$

Here, $A_\pm^\delta = (\sigma_{k,l_1}^\delta \pm \sigma_{k,l_2}^\delta)/2$, $B_\pm^\delta = \sqrt{[JA_-^\delta \pm V_\delta]^2 + t^2}$ and $C_\pm^\delta = \sqrt{2} \sqrt{B_+^\delta (B_+^\delta \pm B_-^\delta) - 2JA_-^\delta V_\delta}$. The lowest-energy eigenstate is then unambiguously determined by the corresponding eigenvector $|\psi\rangle = \prod_{k=1}^N |\psi_k^x\rangle |\psi_k^y\rangle$, which minimizes the overall energy. Of course, the total normalized magnetization m_{tot} of the investigated spin-electron model (1) is given by

$$m_{tot} = \frac{1}{2} \sum_{\delta=x,y} m_{tot}^\delta = \frac{1}{2} \sum_{\delta=x,y} \sum_{k=1}^N \frac{(m_{k,I}^\delta + m_{k,e}^\delta)}{(1 + \langle \hat{n}_k^\delta \rangle)}. \tag{3}$$

For a completeness, the sublattice magnetizations $m_{k,I}^\delta$ and $m_{k,e}^\delta$ of the localized Ising spins and mobile electrons emergent in Eq. (3) are defined as follows

$$\begin{aligned}
m_{k,I}^\delta &= \frac{\langle \hat{\sigma}_{k,l_1}^\delta \rangle + \langle \hat{\sigma}_{k,l_2}^\delta \rangle}{2}, \\
m_{k,e}^\delta &= \sum_{\alpha=1,2} (\langle \hat{n}_{k,l_\alpha,\uparrow}^\delta \rangle - \langle \hat{n}_{k,l_\alpha,\downarrow}^\delta \rangle).
\end{aligned} \tag{4}$$

where $\delta = x, y$.

3. Results and discussion

Before discussing the most interesting results it should be pointed out that all further analyzes will be performed for a ferromagnetic Ising interaction $J > 0$, because the transformation $J \rightarrow -J$ results in a trivial interchange of a relative spin orientation of the mobile electrons with respect to their nearest Ising spins. To reduce a parametric space, we have applied a restriction for a polar angle φ from $\varphi = 0$ to $\varphi = \pi/4$ in all subsequent analyzes, since the higher values of φ only result in symmetry-related magnetic structures obtained by a rotation in xy -plane by the angle $\pi/2$. The restriction to $\langle \hat{n}_k^\delta \rangle \leq 2$ is further applied when taking into account a validity of particle-hole symmetry.

First, let us take a closer look at the particular case without the external magnetic field h/J . Besides three spatially isotropic ground states (A, C and F) already reported in our previous work [25], the non-zero electric field may stabilize other four spatially anisotropic ones (B, D, E and E*), which can be defined through a specific combination of three eigenvectors

$$\begin{aligned}
|0\rangle_k^\delta &= |1\rangle_{\sigma_{k,l_1}} \otimes |0,0\rangle_k \otimes |1\rangle_{\sigma_{k,l_2}} , \\
|\text{I}\rangle_k^\delta &= |1\rangle_{\sigma_{k,l_1}} \otimes \left(\cos a_1^\delta | \uparrow, 0 \rangle_k + \sin a_1^\delta | 0, \uparrow \rangle_k \right) \otimes |1\rangle_{\sigma_{k,l_2}} , \\
\tan a_1^\delta &= \left(\sqrt{V_\delta^2 + t^2} - V_\delta \right) / t , \\
|\text{II}\rangle_k^\delta &= |1\rangle_{\sigma_{k,l_1}} \otimes \left(a_2^\delta | \uparrow, \downarrow \rangle_k + b_2^\delta | \downarrow, \uparrow \rangle_k + c_2^\delta | \uparrow \downarrow, 0 \rangle_k \right. \\
&\quad \left. + d_2^\delta | 0, \uparrow \downarrow \rangle_k \right) \otimes | -1 \rangle_{\sigma_{k,l_2}} , \\
a_2^\delta &= 2t\xi_\delta(\xi_\delta + 2J)/\eta_\delta , \\
b_2^\delta &= -a_2^\delta(\xi_\delta - 2J)/(\xi_\delta + 2J) , \\
c_2^\delta &= a_2^\delta(\xi_\delta - 2J)(\xi_\delta + 2V_\delta)/2t\xi_\delta , \\
d_2^\delta &= c_2^\delta(\xi_\delta - 2V_\delta)/(\xi_\delta + 2V_\delta) , \\
\xi_\delta &= \sqrt{2} \left[(J^2 + V_\delta^2 + t^2) + \left(\frac{(J + V_\delta)^2 + t^2}{((J - V_\delta)^2 + t^2)^{-1}} \right)^{1/2} \right]^{1/2} , \\
\eta_\delta &= \sqrt{2} \left[4t^2\xi_\delta^2(\xi_\delta^2 + 4J^2) + \frac{(\xi_\delta^2 - 4J^2)^2}{(\xi_\delta^2 + 4V_\delta^2)^{-1}} \right]^{1/2} , \\
\delta &= x, y .
\end{aligned} \tag{5}$$

A complete list of all possible ground states is reported in Tab. 1, where individual ground states sorted according to the electron concentration ρ are supplemented with the definition of their notation, ground-state energy (ε_k), the explicit form of the relevant eigenvector ($|\psi\rangle_k$) and the total magnetization (m_{tot}). As one can see, two spatially inho-

ρ	Phase	ε_k	$ \psi\rangle_k$	m_{tot}
0	A	$-h$	$ 0\rangle_k^x 0\rangle_k^y$	1
0.5	B	$-J - 2h - \mu - \omega_x$	$ \text{I}\rangle_k^x 0\rangle_k^y$	1
1	C	$-2J - 3h - 2\mu - \omega_x - \omega_y$	$ \text{I}\rangle_k^x \text{I}\rangle_k^y$	1
1	D	$-h/2 - 2\mu - \Omega_x$	$ \text{II}\rangle_k^x 0\rangle_k^y$	1/2
1.5	E	$-J - 3h/2 - 3\mu - \omega_x - \Omega_y$	$ \text{I}\rangle_k^x \text{II}\rangle_k^y$	1/2
1.5	E*	$-J - 3h/2 - 3\mu - \Omega_x - \omega_y$	$ \text{II}\rangle_k^x \text{I}\rangle_k^y$	1/2
2	F	$-4\mu - \Omega_x - \Omega_y$	$ \text{II}\rangle_k^x \text{II}\rangle_k^y$	0

Table 1: A complete list of all ground states of a coupled spin-electron model on a doubly decorated square lattice for the zero-magnetic-field case. Here $\Omega_{x(y)} = \sqrt{2(J^2 + \omega_{x(y)}^2) + 2\sqrt{(J^2 + \omega_{x(y)}^2)^2 - 4J^2V_{x(y)}^2}}$ and $\omega_{x(y)} = \sqrt{V_{x(y)}^2 + t^2}$.

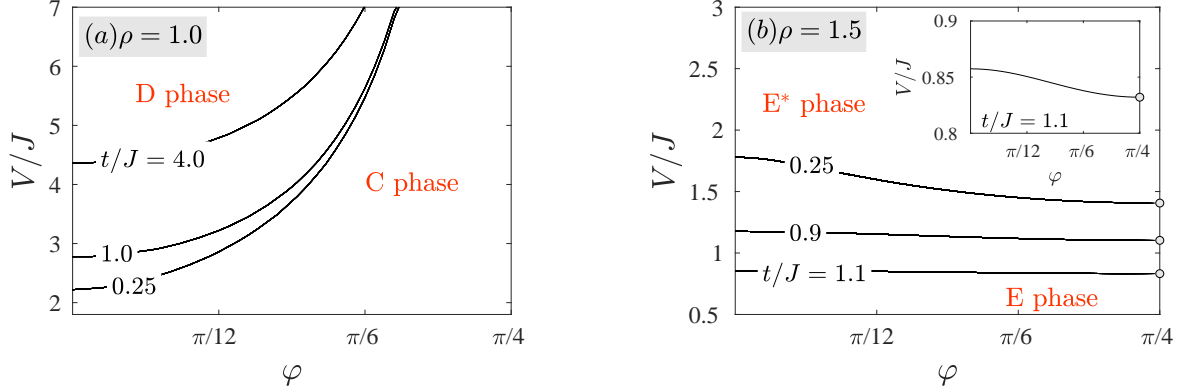


Figure 2: Ground-state phase diagram in the $\varphi - V/J$ plane between two spatially different ground states with the total electron occupation $\rho = 1$ (a) and $\rho = 1.5$ (b) for selected values of the electron hopping t/J in absence of an external magnetic field h/J . Light gray circles in the panel (b) denote the fact that the phases E and E* coexist together for arbitrary V/J if $\varphi = \pi/4$.

homogeneous ground states may exist due to a spatial modulation of the electric field for two electron concentrations $\rho = 1$ and $\rho = 1.5$. The ground-state phase diagrams in the angle versus a relative strength of the electric field ($\varphi - V/J$) plane are presented in Fig. 2. It is evident that phase boundaries between two different ground states exhibit a monotonic but non-constant angular dependence unambiguously demonstrating presence of the rotating magnetoelectric effect. It also follows from Fig. 2 that the rotating magnetoelectric effect significantly depends on a relative strength of the hopping amplitude t/J . While the strengthened hopping amplitude t/J shifts the relevant phase boundary between the ground states C and D to higher values of the electric field V/J at the quarter electron filling ($\rho = 1$), the opposite trend is observed for the phase boundary between the ground states E and E* at the electron concentration $\rho = 1.5$. It is interesting to note that the increasing hopping term t/J reduces for the electron concentration $\rho = 1.5$ the rotating magnetoelectric effect as a consequence of a suppression of the spatially anisotropic phase E. Above the critical value of the electron hopping, numerically identified as $t_c/J \approx 1.305$, the phase E is completely replaced by the phase E* and the rotating magnetoelectric effect completely vanishes. Moreover, the angular change of a spatial orientation of the external electric field ($\varphi < \pi/4$) allows to discontinuously swap magnetic orders of a coupled spin-electron system for the electron concentration $\rho = 1.5$ and relatively weak electron hopping $t/J \lesssim 1.305$ on the horizontal and vertical directions ($E \rightleftharpoons E^*$), in spite of the fact that the total magnetization remains unchanged. For a completeness we note that for the specific orientation of the external electric field $\varphi = \pi/4$ both phases E and E* become energetically equivalent, because the spatial anisotropy vanishes and the energies of the single and doubly occupied bonds are identical for arbitrary strength of the electric field V/J (visualized as the light gray circles in Fig. 2(b)). However, Fig. 3 demonstrates that arbitrary small but non-zero deviation from the most symmetric case $\varphi = \pi/4$ induces the phase transition E-E* at relatively high value of the electric field V/J , on assumption that $t/J \lesssim t_c/J$.

As a next step, let us examine existence of the rotating magnetoelectric effect in presence of the external magnetic field. The situation is in this case much more complex in comparison with a zero-magnetic-field case, because the overall number of ground states increases significantly. Besides the six previously described ground states (given in Tab. 1) we have additionally detected eight different ground states, which can be defined by combination of the eigenvectors given by Eq. (5) and the other two eigenvectors

$$\begin{aligned} |\Pi_2\rangle_k^\delta &= |1\rangle_{\sigma_{k,1}} \otimes (|\uparrow, \uparrow\rangle_k) \otimes |1\rangle_{\sigma_{k,2}}, \\ |\Pi_3\rangle_k^\delta &= |1\rangle_{\sigma_{k,1}} \otimes [a_3^\delta (|\uparrow, \downarrow\rangle_k - |\downarrow, \uparrow\rangle_k) + b_3^\delta |\uparrow, \downarrow, 0\rangle_k \\ &\quad + c_3^\delta |\downarrow, \uparrow, 0\rangle_k] \otimes |1\rangle_{\sigma_{k,2}}, \end{aligned}$$

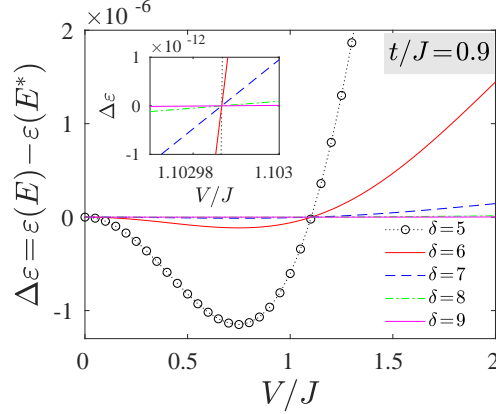


Figure 3: Energy difference $\Delta\varepsilon = \varepsilon(E) - \varepsilon(E^*)$ as a function of the electric field V/J , calculated for $t/J = 0.9$ and $h/J = 0$ for five different angular variables $\varphi = \pi/4 - 1 \times 10^{-\delta}$. Inset shows the details of behaviour in the proximity of the transition electric field V/J .

$$a_3^\delta = \frac{t}{2\sqrt{V_\delta^2 + t^2}}, \quad b_3^\delta = \frac{\sqrt{V_\delta^2 + t^2} + V_\delta}{2\sqrt{V_\delta^2 + t^2}}, \quad c_3^\delta = \frac{\sqrt{V_\delta^2 + t^2} - V_\delta}{2\sqrt{V_\delta^2 + t^2}}. \quad (6)$$

A complete list of eight novel ground states is reported in Tab. 2, where individual ground states are supplemented with the definition of their notation, ground-state energy (ε_k), the explicit form of the relevant eigenvector ($|\psi\rangle_k$) and the total magnetization (m_{tot}). It can be shown that more than one possible ground state may emerge for any out of three considered electron concentrations $\rho = 1.0, 1.5$ and 2.0 . Therefore, the existence of the rotating magnetoelectric effect under presence of the external magnetic field could be expected. The ground-state phase diagrams in the angle versus a relative strength of the electric field ($\varphi - V/J$) plane under the influence of the non-zero magnetic field h/J are presented in Figs. 4-6. In agreement with general expectations the applied magnetic field stabilizes the ferromagnetic structures instead of the antiferromagnetic one at a quarter filling ($\rho = 1$), whereas the relevant ground-state phase boundaries depend monotonically on the angular variable φ (see Fig. 4). Consequently, the applied magnetic field preserves the rotating magnetoelectric effect at a quarter electron filling, however, it shifts its occurrence to the higher value of the electric field V/J .

ρ	Phase	ε_k	$ \psi\rangle_k$	m_{tot}
1	G	$-h - 2\mu - 2\omega_x$	$ \Pi_3\rangle_k^x 0\rangle_k^y$	2/3
1.5	H	$-J - 2h - 3\mu - 2\omega_x - \omega_y$	$ \Pi_3\rangle_k^x \Pi_3\rangle_k^y$	2/3
1.5	I	$-3J - 4h - 3\mu - \omega_x$	$ \Pi_1\rangle_k^x \Pi_2\rangle_k^y$	1
2	J	$-2J - 5h/2 - 4\mu - \Omega_x$	$ \Pi_1\rangle_k^x \Pi_2\rangle_k^y$	1/2
2	K	$-h/2 - 4\mu - 2\omega_x - \Omega_y$	$ \Pi_3\rangle_k^x \Pi_3\rangle_k^y$	1/6
2	L	$-2J - 3h - 4\mu - 2\omega_x$	$ \Pi_3\rangle_k^x \Pi_2\rangle_k^y$	2/3
2	M	$-h - 4\mu - 2\omega_x - 2\omega_y$	$ \Pi_3\rangle_k^x \Pi_3\rangle_k^y$	1/3
2	N	$-4J - 5h - 4\mu$	$ \Pi_2\rangle_k^x \Pi_2\rangle_k^y$	1

Table 2: A list of additional eight ground states of a coupled spin-electron model on a doubly decorated square lattice emergent due to presence of the external magnetic field. Here $\Omega_{x(y)} = \sqrt{2(J^2 + \omega_{x(y)}^2) + 2\sqrt{(J^2 + \omega_{x(y)}^2)^2 - 4J^2V_{x(y)}^2}}$ and $\omega_{x(y)} = \sqrt{V_{x(y)}^2 + t^2}$.

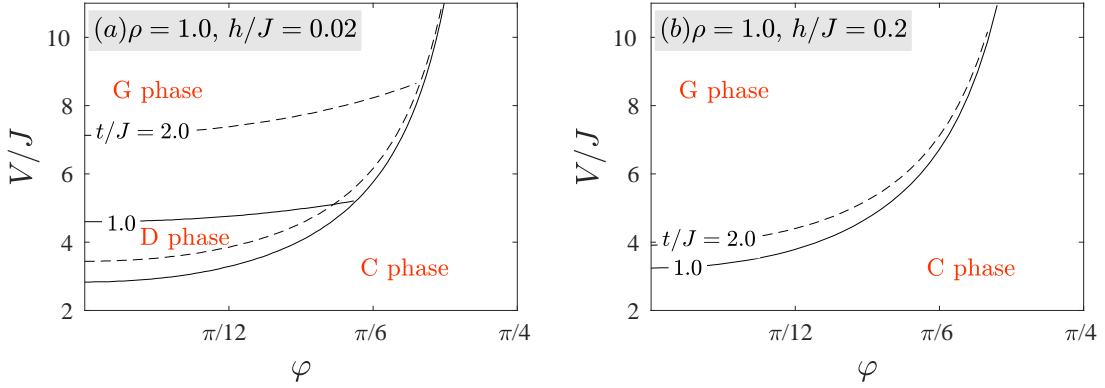


Figure 4: Ground-state phase diagram in the $\varphi - V/J$ plane at a quarter filling $\rho=1.0$ for two different values of the external magnetic field $h/J=0.02$ (a) and 0.2 (b) and two different values of the hopping amplitude $t/J=1.0$ (solid lines) and $t/J=2.0$ (dashed lines).

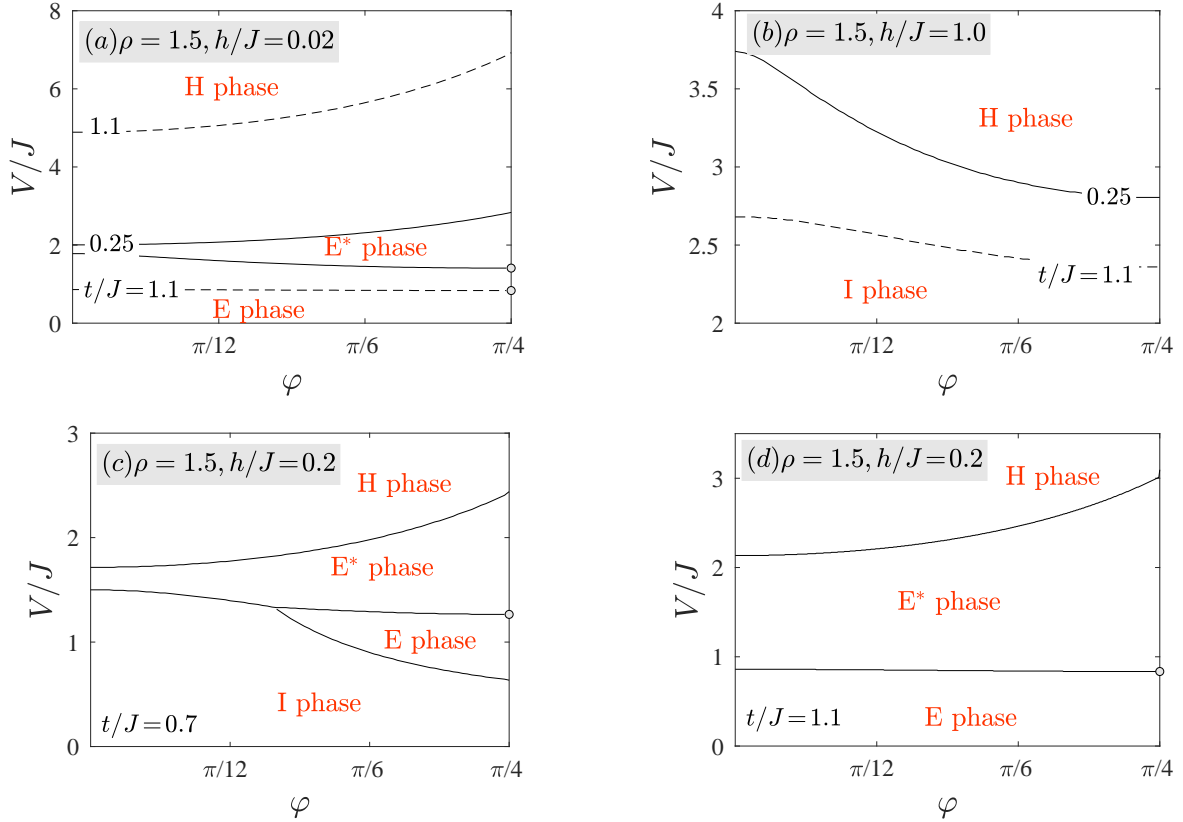


Figure 5: Ground-state phase diagram in the $\varphi - V/J$ plane at a fractional electron filling $\rho=1.5$ for three different values of the external magnetic field $h/J=0.02$ (a), 1.0 (b) and 0.2 (c)-(d). Different values of the hopping amplitude t/J are taken into account. Light gray circles in panels (a), (c) and (d) denote the fact that the phases E and E* coexist together for arbitrary V/J if $\varphi=\pi/4$.

The investigated system at the mean electron concentration $\rho=1.5$ can exhibit at most three zero-temperature phase transitions driven by the electric field V/J , which may result in four different types of ground-state phase diagrams

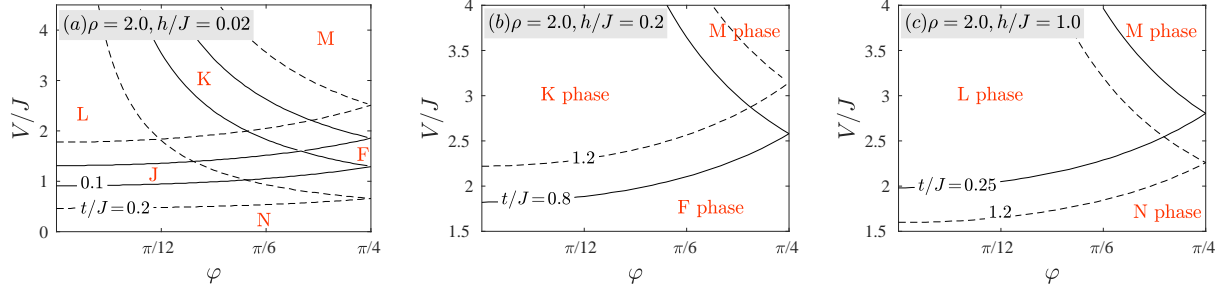


Figure 6: Ground-state phase diagram in the $\varphi - V/J$ plane at a half filling $\rho = 2.0$ for three different values of the external magnetic field $h/J = 0.02$ (a), 0.2 (b) and 1.0 (c). Different values of the hopping amplitude t/J are taken into account.

shown in Fig. 5. It was found that the magnetic field dominantly influences the spin subsystem, which becomes ferromagnetic, although the changes in the electron subsystem strongly depend on a magnitude of the applied electric field. Similarly as in the previous case ($\rho = 1$), the non-negligible effect of a polar angle φ determining a spatial orientation of the external electric field on a stability of the relevant ground states is also evident for the particular case $\rho = 1.5$. Moreover, the obtained phase diagrams at non-zero magnetic field $h/J \neq 0$ and $\varphi < \pi/4$ demonstrate that the unconventional phenomenon of swapping magnetic orders on the horizontal and vertical direction ($E \rightleftharpoons E^*$) is dramatically reduced upon the applied magnetic field. However a complete suppression of this phenomenon is detected just above a relatively large magnetic field $h/J \approx 0.9$.

In the most interesting half-filled case $\rho = 2$ the rotating magnetoelectric effect is substantially influenced by a competition of both applied fields, because the non-zero magnetic field favors six different ground states instead of a single ground state F detected in zero-magnetic-field case. Under this condition, there are three possible types of ground-state phase diagrams as illustrated Fig. 6. The most diverse ground-state phase diagram can be found at very low magnetic fields, where the competition between the isotropic and anisotropic tendency of the magnetic and electric fields leads to the existence of six different phases. Of course, the phase boundaries between the individual ground states are substantially affected by the hopping term t/J , which generally stabilizes spatially anisotropic structures instead of the isotropic ones. With no exception, all phase boundaries exhibit a monotonic angular dependence demonstrating presence of the rotating magnetoelectric effect. The higher values of the magnetic field h/J as well as the hopping amplitude t/J reduce the overall structure of the ground-state phase diagram due to suppression of some phases. While the competing effect of moderate magnetic field (e.g. $h/J = 0.2$) and the applied electric field still preserves the electron segregation over the horizontal and vertical bonds, the sufficiently strong magnetic field (e.g. $h/J = 1.0$) reorients spins into its direction and the homogeneous distribution of electrons becomes energetically favourable. In all identified phase boundaries the influence of the polar angle φ specifying a spatial orientation of the external electric field is evident, and thus existence of the rotating magnetoelectric effect is observed.

4. Conclusion

The ground-state properties of a coupled spin-electron model on a doubly decorated square lattice have been investigated under the influence of the external electric field acting either separately or in a mutual competition with an external magnetic field. The main goal was to study presence of the intriguing rotating magnetoelectric effect achieved upon the sample rotation in a homogeneous external electric field. It was found that the dissimilar impact of the electric field on the electron subsystems in the horizontal and vertical directions produces novel inhomogeneous magnetic ground states, which become dominant upon increasing a relative strength of the electrostatic potential and/or decreasing the polar angle determining the spatial orientation of the external electric field. Due to this spatial anisotropy, the investigated spin-electron system in absence of an external magnetic field can exhibit two different ground states for the electron concentrations $\rho = 1$ and $\rho = 1.5$. A monotonic (non-constant) character of a discontinuous phase transition between two respective ground states driven by a spatial orientation of the electric field directly confirms

presence of a rotating magnetoelectric effect in a coupled spin-electron system on a doubly decorated square lattice. It turns out that the rotating magnetoelectric effect also persists for both aforementioned electron concentrations ($\rho = 1$ and $\rho = 1.5$) in presence of the external magnetic field, which in addition generates novel spatially anisotropic ground states. It was shown that the phase boundaries among all novel phases very sensitively depend on the polar angle φ specifying a spatial orientation of the external electric field, what equally demonstrates presence of the rotating magnetoelectric effect. In addition, it was found that presence of an arbitrarily small but non-zero magnetic field at a half filling $\rho = 2$ generates at most five novel ground states depending on a relative strength of the magnetic field h/J and the hopping term t/J . A monotonic dependence of detected phase boundaries between each two coexisting phases on the polar angle φ confirm existence of the rotating magnetoelectric effect also in the physically most interesting half-filled case $\rho = 2$. It should be emphasized that this effect is a direct consequence of a competition between both applied external fields (magnetic as well as electric) and cannot exist in absence of one of them. Besides, the variation of the polar angle $\varphi < \pi/4$ can produce another interesting behavior, exclusively observed at the fractional electron concentration $\rho = 1.5$ and a relative weak hopping term t/J , where the magnetic orders of the spin-electron system on a doubly decorated square lattice can be easily swapped on the horizontal and vertical direction ($E \rightleftharpoons E^*$). Although the strengthening of the magnetic field significantly reduces this phenomenon, it is necessary to apply sufficiently strong magnetic fields $h/J \approx 0.9$ to fully suppress this swapping. Without any doubts, the aforementioned diversity makes such spin-electron systems very attractive for a possible application in spintronics, sensorics or storage devices.

This work was supported by the Slovak Research and Development Agency (APVV) under Grant No. APVV-16-0186. The financial support provided by the VEGA under Grant No. 1/0105/20 is also gratefully acknowledged.

References

- [1] M. Fiebig, *J. Phys. D* **38**, R123 (2005).
- [2] S. A. Nikitin, K. P. Skokov, Y. S. Koshkidko, Y. G. Pastushenkov, and T. I. Ivanova, *Phys. Rev. Lett.* **105** (2010) 137205.
- [3] Y. Tokura, S. Seki, and N. Nagaosa, *Rep. Prog. Phys.* **77** (2014) 076501.
- [4] M. S. Cao, X. X. Wang, M. Zhang, J. Ch. Shu, W. Q. Cao, H. J. Yang, X. Y. Fang, and J. Yuan, *Adv. Funct. Mater.* **29** (2019) 1807398.
- [5] G. A. Prinz, *Science* **282** (1998) 1660.
- [6] S. A. Wolf, D. D. Awschalom, R. A. Buhrman, J. M. Daughton, S. von Molnár, M. L. Roukes, A. Y. Chtchelkanova, and D. M. Treger, *Science* **294** (2001) 1488.
- [7] J. Y. Son, J.-H. Lee, S. Song, Y.-H. Shin, and H. M. Jang, *ACS Nano* **7** (2013) 5522.
- [8] J. F. Scott, *Nat. Mater.* **6** (2007) 256.
- [9] N. Hur, S. Park, P. A. Sharma, J. S. Ahn, S. Guha, and S.-W. Cheong, *Nature* **429** (2004) 392.
- [10] S. M. Wu, S. A. Cybart, P. Yu, M. D. Rossell, J. X. Zhang, R. Ramesh, and R. C. Dynes, *Nat. Mater.* **9** (2010) 756.
- [11] M. M. Vopson, *Crit. Rev. Solid State* **40** (2015) 223.
- [12] G. Sreenivasulu, P. Qu, V. Petrov, H. Qu, and G. Srinivasan, *Sensors* **16** (2016) 262.
- [13] H. Čenčariková and J. Strečka, *Phys. Lett. A* **383** (2019) 125957.
- [14] H. Zhang, Y. W. Li, E. K. Liu, Y. J. Ke, J. L. Jin, Y. Long, and B. G. Shen, *Sci. Rep.* **5** (2015) 11929.
- [15] J. Caro Pantino and N. A. de Oliveira, *Intermetallics* **64** (2015) 59.
- [16] G. Lorusso, O. Roubeau, M. Evangelisti, *Angew. Chem.* **55** (2016) 3360.
- [17] M. Balli, S. Jandl, P. Fournier, and F. Z. Dimitrov, *Appl. Phys. Lett.* **108** (2016) 102401.
- [18] M. Balli, S. Jandl, P. Fournier, and A. Kedous-Lebouc, *Appl. Phys. Rev.* **4** (2017) 021305.
- [19] M. Orendáč, S. Gabáni, E. Gažo, G. Pristáš, N. Shitsevalova, K. Siemensmeyer, and K. Flachbart, *Sci. Rep.* **8** (2018) 10933.
- [20] J. Y. Moon, M. K. Kim, D. G. Oh, J. H. Kim, H. J. Shin, Y. J. Choi, and N. Lee, *Phys. Rev. B* **98** (2018) 174424.
- [21] H. Čenčariková, J. Strečka, and A. Gendiar, *J. Magn. Magn. Mater.* **452** (2018) 512.
- [22] H. Čenčariková, J. Strečka, and M. L. Lyra, *J. Magn. Magn. Mater.* **401** (2016) 1106.
- [23] H. Čenčariková and J. Strečka, *Phys. Rev. E* **98** (2018) 062129.
- [24] H. Čenčariková, J. Strečka, A. Gendiar, and N. Tomašovičová, *Physica B* **536** (2018) 432.
- [25] J. Strečka, H. Čenčariková, M. L. Lyra, *Phys. Lett. A* **379** (2015) 2915.